# Simultaneous monitoring of monoclonal antibody variants by strong cation-exchange chromatography hyphenated to mass spectrometry to assess critical attributes of rituximab-based biotherapeutics

**Fiammetta Di Marco [1,2], Thomas Berger [1,2], Wolfgang Esser-Skala[1,2,3], Erdmann Rapp[4,5], Christof Regl[1,2] and Christian Huber [1,2,*]**

[1] Department of Biosciences, Bioanalytical Research Labs, University of Salzburg, Hellbrunner Straße 34, 5020 Salzburg, Austria
[2] Christian Doppler Laboratory for Innovative Tools for Biosimilar Characterization, University of Salzburg, Hellbrunner Straße 34, 5020 Salzburg, Austria
[3] Department of Biosciences, Computational Systems Biology Group, University of Salzburg, Hellbrunner Straße 34, 5020 Salzburg, Austria
[4] glyXera GmbH, Brenneckestraße 20 - ZENIT, 39120 Magdeburg, Germany
[5] Max Planck Institute for Dynamics of Complex Technical Systems, Sandtorstraße 1, 39106 Magdeburg, Germany
* Correspondence: c.huber@sbg.ac.at

**Table of Contents**

**Supplementary Figures**

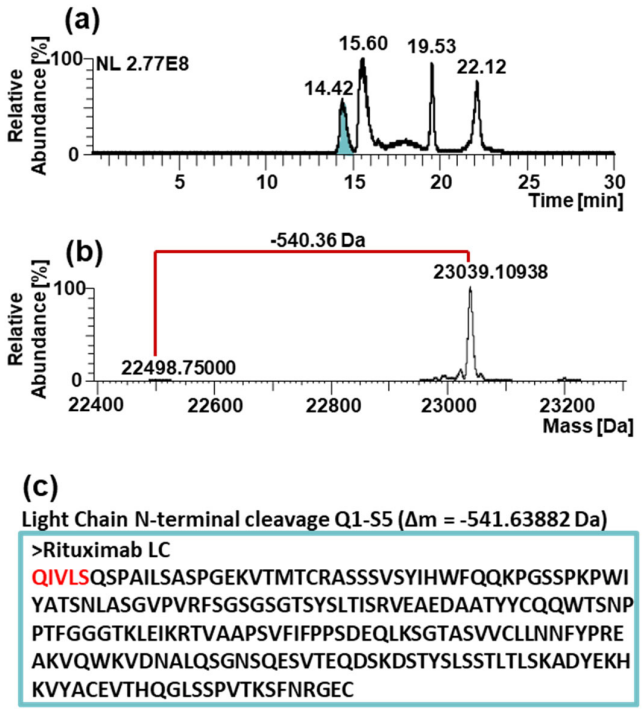


**Figure S1. (a)** Chromatogram of reduced Reditux™ (5 mM TCEP) obtained by RP-HPLC-MS analysis. Heavy and light chains are dissociated due to the reducing condition and separated by RP-HPLC. **(b)** Deconvoluted mass spectrum of the light chain corresponding to chromatographic peak at 14.42 min (highlighted in light blue). A variant differing in mass by -540.36 Da (22498.75000 Da) can be observed in the spectrum. (**c**) Rituximab light chain sequence. The variant at 22498.75000 Da could arise from cleavage of the first five residues (Q1-S5, indicated in red) of the light chain N-terminus resulting in a Δm of -541.63882 Da.

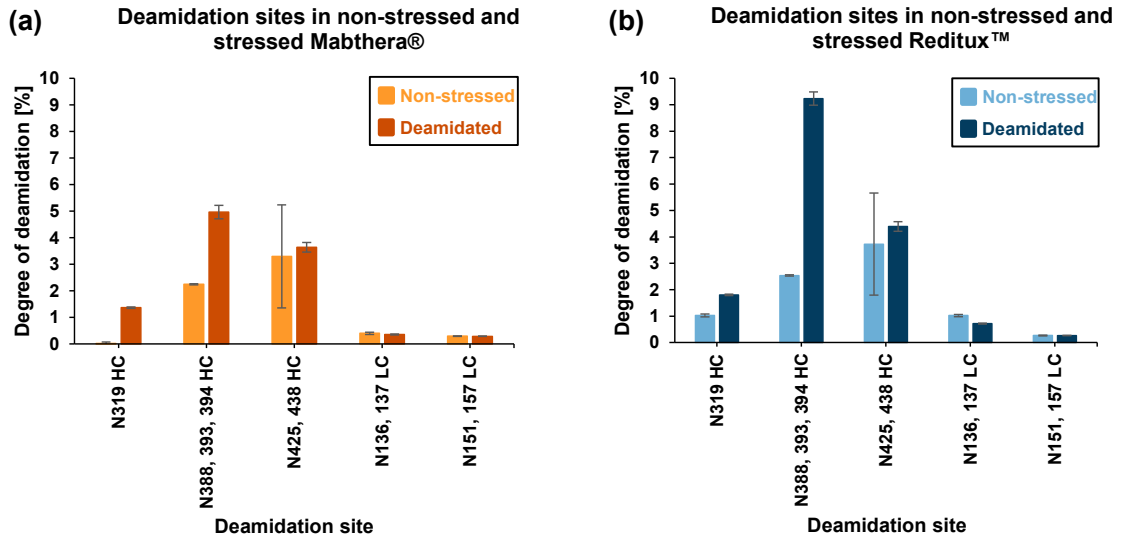


**(c)**

**>Rituximab HC**
QVQLQQPGAELVKPGASVKMSCKASGYTFTSYNMHWVKQTPGRGLEWIGAIYPGNGDTSYNQKFKGKATLTADKSSSTAYMQLSSLTSEDSAVYYCARSTYYGGDWY
FNVWGAGTTVTVSAASTKGPSVFPLAPSSKSTSGGTAALGCLVKDYFPEPVTVSWNSGALTSGVHTFPAVLQSSGLYSLSSVVTVPSSSLGTQTYICNVNHKPSNTKVDKK
AEPKSCDKTHTCPPCPAPELLGGPSVFLFPPKPKDTLMISRTPEVTCVVVDVSHEDPEVKFNWYVDGVEVHNAKTKPREEQYNSTYRVVSVLTVLHQDWL$N_{319}$GKEYKCK
VSNKALPAPIEKTISKAKGQPREPQVYTLPPSRDELTKNQVSLTCLVKGFYPSDIAVEWES$N_{388}$GQPE$N_{393}$$N_{394}$YKTTPPVLDSDGSFFLYSKLTVDKSRWQQG$N_{425}$VFSCS
VMHEALH$N_{438}$HYTQKSLSLSPGK
**>Rituximab LC**
QIVLSQSPAILSASPGEKVTMTCRASSSVSYIHWFQQKPGSSPKPWIYATSNLASGVPVRFSGSGSGTSYSLTISRVEAEDAATYYCQQWTSNPPTFGGGTKLEIKRTVAAP
SVFIFPPSDEQLKSGTASVVCLL$N_{136}$$N_{137}$FYPREAKVQWKVD$N_{151}$ALQSG$N_{157}$SQESVTEQDSKDSTYSLSSTLTLSKADYEKHKVYACEVTHQGLSSPVTKSFNRGEC

**Figure S2.** Bar charts of peptide deamidation degree in **(a)** control and forced deamidated MabThera®, **(b)** non-stressed and forced deamidated Reditux™. Deamidation sites are indicated with residue position and the corresponding subunits (Heavy Chain, HC or Light Chain, LC) in the x-axis. Quantitation of peptide was based on peak integration of EICCs of MS1 ions in peptide mapping data, thus asparagine residues are considered together when belonging to the same peptide. **(c)** Rituximab amino acid sequence with deamidation sites reported in red.

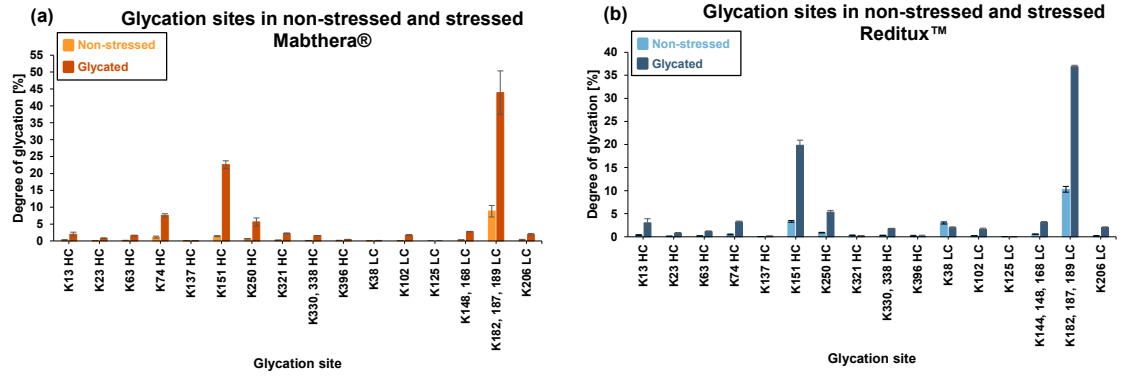


**(c)**

**>Rituximab HC**

QVQLQQPGAELV$K_{13}$PGASVKMSC$K_{23}$ASGYTFTSYNMHWVKQTPGRGLEWIGAIYPGNGDTSYNQ$K_{63}$FKGKATLTAD$K_{74}$SSTAYMQLSSLTSEDSAVYYCARSTYYGGDWYFNVWGA
GTTVTVSAASTKGPSVFPLAPSS$K_{137}$STSGGTAALGCLV$K_{151}$DYFPEPVTVSWNSGALTSGVHTFPAVLQSSGLYSLSSVVTVPSSSLGTQTYICNVNHKPSNTKVDKKAEPKSCDKTHTCPPC
PAPELLGGPSVFLFPP$K_{250}$PKDTLMISRTPEVTCVVVDVSHEDPEVKFNWYVDGVEVHNAKTKPREEQYNSTYRVVSVLTVLHQDWLNG$K_{321}$EYKCKVSN$K_{330}$ALPAPIE$K_{338}$TISKAKGQ
PREPQVYTLPPSRDELTKNQVSLTCLVKGFYPSDIAVEWESNGQPENNY$K_{396}$TTPPVLDSDGSFFLYSKLTVDKSRWQQGNVFSCSVMHEALHNHYTQKSLSLSPGK

**>Rituximab LC**

QIVLSQSPAILSASPGEKVTMTCRASSSVSYIHWFQQ$K_{38}$PGSSPKPWIYATSNLASGVPVRFSGSGSGTSYSLTISRVEAEDAATYYCQQWTSNPPTFGGGT$K_{102}$LEIKRTVAAPSVFIFPPSD
EQLK$_{125}$SGTASVVCLLNNFYPREA$K_{144}$VQW$K_{148}$VDNALQSGNSQESVTEQDS$K_{168}$DSTYSLSSTLTLS$K_{182}$ADYE$K_{187}$H$K_{189}$VYACEVTHQGLSSPVT$K_{206}$FNRGEC

**Figure S3.** Bar charts of peptide glycation degree in **(a)** control and forced glycated MabThera®, **(b)** non-stressed and forced glycated Reditux™. Glycation sites are indicated with residue position and the corresponding subunits (Heavy Chain, HC or Light Chain, LC) in the x-axis. Quantitation of peptide was based on peak integration of EICCs of MS1 ions in peptide mapping data, thus lysine residues are considered together when belonging to the same peptide. **(c)** Rituximab amino acid sequence with glycation sites reported in red.

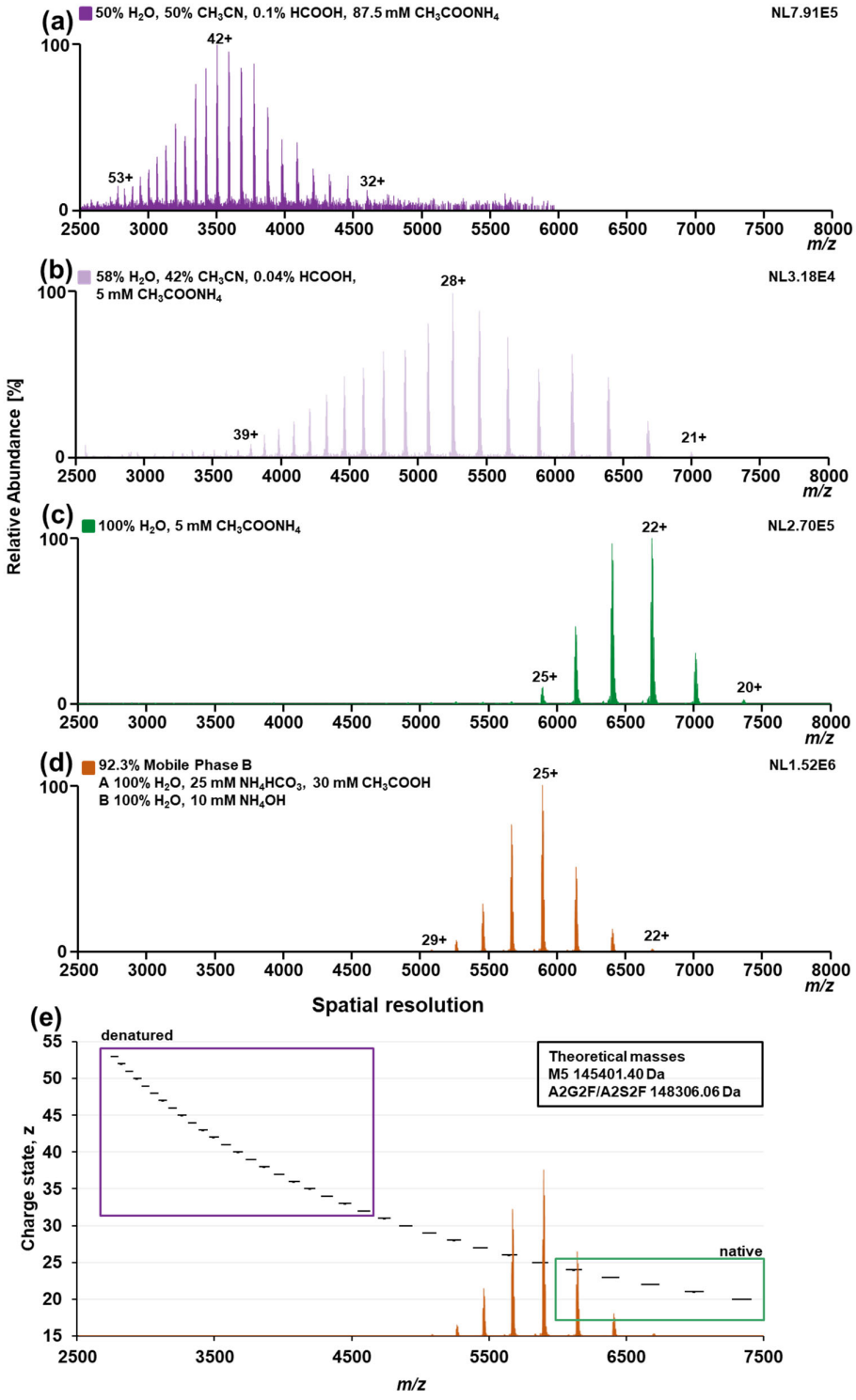


**Figure S4.** Direct infusion MS analyses of MabThera® in **(a)** a denaturing solution, **(b)** a partially denaturing solution,**(c)** a solution maintaining the mAb in the quasi-native state. **(d)** SCX-HPLC-MS analysis of MabThera® eluting at 92.3% Mobile Phase B (A: 100% $H_2O$, 25 mM $NH_4HCO_3$, 30 mM $CH_3COOH$, B: 100% $H_2O$, 10 mM $NH_4OH$). **(e)** Charge state dependent spatial resolution plot. Charge envelope range were calculated considering the theoretical masses of the first (M5, 145401.40 Da) and the last (A2G2F/A2S2F, 148306.06 Da) glycoform observed. The charge envelope partially overlaps going towards higher charge state (denaturing condition). The mass spectrum of MabThera® acquired by SCX-HPLC-MS analysis (orange) is in quasi- native charge range.

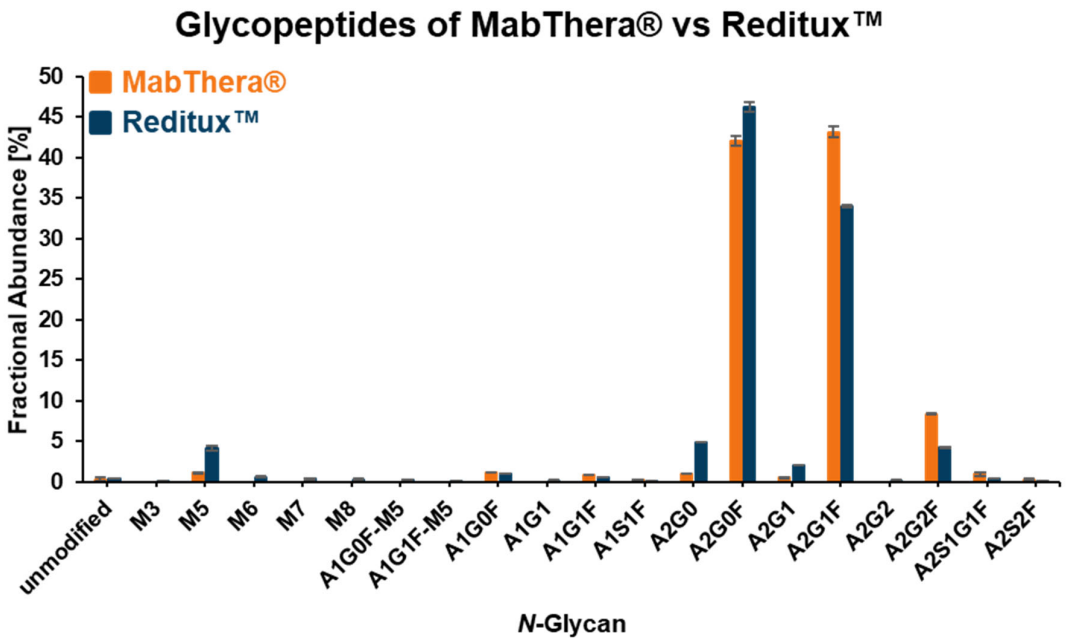


**Figure S5.** Bar chart reporting *N*-glycans fractional abundances obtained by nano-RPLC-MS/MS of glycopeptides of MabThera® (orange) and Reditux™ (blue). MabThera® showed a higher degree of sialylation and galactosylation compared to Reditux™ that exhibited instead a higher abundance of oligomannose and afucosylated variants. Glycan structures, names and compositions are collected in Table S1.

**Supplementary Tables**

**Table S1.** Name, structure and monosaccharide composition of MabThera® and Reditux™ *N*-glycans elucidated by xCGE-LIF. A green cell indicates presence, a red cell absence of that glycan in the drug product.

| N-Glycans | | | | |
|---|---|---|---|---|
| Name | Structure | Monosaccharide composition | MabThera® | Reditux™ |
| M3 |  | HexNac(2)Hex(3)Neu5Ac(0)Fuc(0) | | |
| M5 |  | HexNac(2)Hex(5)Neu5Ac(0)Fuc(0) | | |
| M6 |  | HexNac(2)Hex(6)Neu5Ac(0)Fuc(0) | | |
| M7 |  | HexNac(2)Hex(7)Neu5Ac(0)Fuc(0) | | |
| M8 | 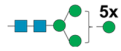 | HexNac(2)Hex(8)Neu5Ac(0)Fuc(0) | | |
| A1G0F-M5 |  | HexNac(3)Hex(5)Neu5Ac(0)Fuc(1) | | |
| A1G1F-M5 |  | HexNac(3)Hex(6)Neu5Ac(0)Fuc(1) | | |
| A1G0F |  | HexNac(3)Hex(3)Neu5Ac(0)Fuc(0) | | |
| A1G1 |  | HexNac(3)Hex(4)Neu5Ac(0)Fuc(0) | | |
| A1G1F |  | HexNac(3)Hex(4)Neu5Ac(0)Fuc(1) | | |
| A1S1F | 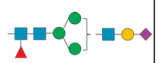 | HexNac(3)Hex(4)Neu5Ac(1)Fuc(1) | | |
| A2G0 |  | HexNac(4)Hex(3)Neu5Ac(0)Fuc(0) | | |
| A2G0F |  | HexNac(4)Hex(3)Neu5Ac(0)Fuc(1) | | |
| A2G1 | 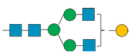 | HexNac(4)Hex(4)Neu5Ac(0)Fuc(0) | | |
| A2G1F |  | HexNac(4)Hex(4)Neu5Ac(0)Fuc(1) | | |
| A2G2 | 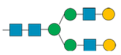 | HexNac(4)Hex(5)Neu5Ac(0)Fuc(0) | | |
| A2G2F | 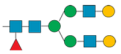 | HexNac(4)Hex(5)Neu5Ac(0)Fuc(1) | | |
| A2S1G1F | 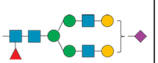 | HexNac(4)Hex(5)Neu5Ac(1)Fuc(1) | | |
| A2S2F |  | HexNac(4)Hex(5)Neu5Ac(2)Fuc(1) | | |

**Table S2.** Glycoform annotation of the deconvoluted mass spectrum of MabThera® (Figure 1b and 4) reporting variant name, experimental mass, theoretical mass, mass deviation in ppm, fractional abundance, retention time range and retention time apex. Theoretical masses were calculated considering N-terminal pyro-Glu as a fixed modification. Glycan structures, names and compositions are collected in Table S1.

| | MabThera® annotation | | | | | |
|---|---|---|---|---|---|---|
| Variant Name | Experimental Mass [Da] | Theoretical Mass [Da] | Mass deviation [ppm] | Fractional Abundance [%] | RT range [min] | RT apex [min] |
| M5_0K | 145411.05 | 145401.40 | 66.3 | 0.01 | 9.98 - 12.03 | 11.52 |
| A2G0F_0K | 145631.87 | 145629.65 | 15.3 | 0.19 | 9.24 - 12.03 | 11.52 |
| A2G1F_0K | 145792.49 | 145791.79 | 4.8 | 0.22 | 8.98 - 12.03 | 10.73 |
| A2G2F_0K | 145953.88 | 145953.93 | -0.3 | 0.09 | 8.98 - 12.03 | 11.52 |
| unidentified | 146252.17 | | | 0.00 | 9.50 - 11.24 | 10.49 |
| unidentified | 146508.84 | | | 0.01 | 9.98 - 11.50 | 11.00 |
| M5/M5_0K | 146623.72 | 146618.49 | 35.6 | 0.40 | 9.77 - 12.03 | 11.52 |
| A2G0/M5_0K | 146703.51 | 146700.60 | 19.8 | 0.02 | 9.24 - 12.03 | 11.52 |
| A2G1/M5_0K | 146858.12 | 146862.74 | -31.4 | 0.09 | 8.98 - 12.03 | 11.52 |
| A2G0/A2G0F_0K | 146926.13 | 146928.84 | -18.5 | 0.08 | 8.98 - 12.03 | 11.52 |
| A2G0F/A2G0F_0K | 147076.43 | 147074.99 | 9.9 | 19.02 | 8.98 - 12.03 | 11.52 |
| A2G0F/A2G1F_0K | 147236.40 | 147237.13 | -4.9 | 32.85 | 8.98 - 12.03 | 11.52 |
| A2G1F/A2G1F_0K or A2G0F/A2G2F_0K | 147397.94 | 147399.27 | -9.0 | 28.85 | 8.98 - 12.03 | 11.26 |
| A2G1F/A2G2F_0K | 147559.97 | 147561.41 | -9.7 | 14.16 | 8.98 - 12.03 | 11.26 |
| A2G2F/A2G2F_0K | 147720.06 | 147723.55 | -23.6 | 1.81 | 8.98 - 12.03 | 11.26 |
| A2G1F/A2S1G1F_0K | 147855.90 | 147852.66 | 21.9 | 0.75 | 8.98 - 12.03 | 10.01 |
| A2G2F/A2S1G1F_0K | 148012.41 | 148014.80 | -16.2 | 0.19 | 9.50 - 11.77 | 10.26 |
| A2G1F/A2S2F_0K | 148146.29 | 148143.92 | 16.0 | 0.37 | 8.98 - 12.03 | 9.48 |
| A2G2F/A2S2F_0K | 148306.06 | 148306.06 | 0.0 | 0.17 | 8.98 - 11.00 | 9.48 |
| unidentified | 148474.93 | | | 0.01 | 8.98 - 10.76 | 9.48 |
| unidentified | 148681.42 | | | 0.01 | 9.77 - 11.77 | 10.73 |
| unidentified | 148842.84 | | | 0.01 | 9.77 - 11.24 | 10.49 |
| unidentified | 148944.16 | | | 0.00 | 9.50 - 12.03 | 11.52 |

**Table S3.** Glycoform annotation of the deconvoluted mass spectrum of MabThera® after carboxypeptidase B (CpB) treatment (Figure 1b) reporting variant name, experimental mass, theoretical mass, mass deviation in ppm, fractional abundance, retention time range and retention time apex. Theoretical masses were calculated considering N-terminal pyro-Glu as a fixed modification. Glycan structures, names and compositions are collected in Table S1.

| MabThera® CpB annotation | | | | | | |
|---|---|---|---|---|---|---|
| Variant Name | Experimental Mass [Da] | Theoretical Mass [Da] | Mass deviation [ppm] | Fractional Abundance [%] | RT range [min] | RT apex [min] |
| A2G0F_0K | 145631.55 | 145629.65 | 13.0 | 0.17 | 10.21 - 12.01 | 11.76 |
| A2G1F_0K | 145793.74 | 145791.79 | 13.4 | 0.35 | 9.21 - 12.01 | 11.76 |
| A2G2F_0K | 145955.01 | 145953.93 | 7.4 | 0.11 | 10.21 - 12.01 | 11.76 |
| unidentified | 146506.88 | | | 0.02 | 11.16 - 12.01 | 11.76 |
| M5/M5_0K | 146623.46 | 146618.49 | 33.9 | 0.21 | 10.32 - 12.01 | 11.76 |
| A2G1/M5_0K | 146856.08 | 146862.74 | -45.4 | 0.13 | 9.37 - 12.01 | 11.76 |
| A2G0/A2G0F_0K | 146926.51 | 146928.84 | -15.9 | 0.23 | 9.37 - 12.01 | 11.76 |
| A2G0F/A2G0F_0K | 147076.55 | 147074.99 | 10.7 | 18.11 | 9.00 - 12.01 | 11.76 |
| A2G0F/A2G1F_0K | 147236.80 | 147237.13 | -2.2 | 31.67 | 9.00 - 12.01 | 11.76 |
| A2G1F/A2G1F_0K or A2G0F/A2G2F_0K | 147398.38 | 147399.27 | -6.0 | 28.75 | 9.00 - 12.01 | 11.76 |
| A2G1F/A2G2F_0K | 147561.21 | 147561.41 | -1.3 | 13.53 | 9.00 - 12.01 | 11.76 |
| A2G2F/A2G2F_0K | 147722.43 | 147723.55 | -7.6 | 1.61 | 9.00 - 12.01 | 11.76 |
| A2G1F/A2S1G1F_0K | 147856.73 | 147852.66 | 27.5 | 1.56 | 9.21 - 11.75 | 11.15 |
| A2G2F/A2S1G1F_0K | 148014.33 | 148014.80 | -3.2 | 0.42 | 9.11 - 12.01 | 11.15 |
| A2G1F/A2S2F_0K | 148147.29 | 148143.92 | 22.7 | 0.74 | 9.00 - 11.88 | 10.55 |
| A2G2F/A2S2F_0K | 148308.14 | 148306.06 | 14.0 | 0.41 | 9.11 - 11.66 | 10.56 |

**Table S4.** Glycoform annotation of the deconvoluted mass spectra of Reditux™ (Figure 1c-e) reporting variant name, experimental mass, theoretical mass, mass deviation in ppm, fractional abundance, retention time range and retention time apex. Theoretical masses were calculated considering N-terminal pyro-Glu as a fixed modification. Glycan structures, names and compositions are collected in Table S1.

| | Reditux™ annotation | | | | | |
|---|---|---|---|---|---|---|
| Variant Name | Experimental Mass [Da] | Theoretical Mass [Da] | Mass deviation [ppm] | Fractional Abundance [%] | RT range [min] | RT apex [min] |
| M5_0K | 145410.20 | 145401.40 | 60.5 | 0.08 | 11.50 - 12.47 | 12.32 |
| A2G0F_0K | 145631.75 | 145629.65 | 14.4 | 0.19 | 11.50 - 12.47 | 12.01 |
| A2G1F_0K | 145790.19 | 145791.79 | -11.0 | 0.20 | 11.50 - 12.47 | 12.01 |
| A2G2F_0K | 145948.23 | 145953.93 | -39.0 | 0.03 | 11.50 - 12.03 | 11.64 |
| A2S1G0F_0K | 146094.50 | 146083.05 | 78.4 | 0.11 | 11.50 - 12.47 | 12.32 |
| unidentified | 146254.66 | | | 0.00 | 11.50 - 12.26 | 11.64 |
| M5/M5_0K | 146620.97 | 146618.49 | 16.9 | 3.87 | 11.50 - 12.47 | 12.1 |
| A2G0/A2G0_0K | 146790.01 | 146782.70 | 49.8 | 0.53 | 11.50 - 12.32 | 11.8 |
| A2G0/A2G0F_0K | 146924.44 | 146928.84 | -29.9 | 3.63 | 11.50 - 12.47 | 11.88 |
| A2G0F/A2G0F_0K | 147077.94 | 147074.99 | 20.1 | 29.80 | 11.50 - 12.47 | 11.95 |
| A2G0F/A2G1F_0K | 147239.24 | 147237.13 | 14.4 | 34.70 | 11.50 - 12.47 | 11.88 |
| A2G1F/A2G1F_0K or A2G0F/A2G2F_0K | 147400.26 | 147399.27 | 6.7 | 21.63 | 11.50 - 12.47 | 11.88 |
| A2G1F/A2G2F_0K | 147560.25 | 147561.41 | -7.8 | 3.61 | 11.50 - 12.16 | 11.71 |
| A2G2F/A2G2F_0K | 147708.05 | 147723.55 | -104.9 | 0.49 | 11.50 - 12.16 | 11.64 |
| A2G1F/A2S1G1F_0K | 147856.13 | 147852.66 | 23.4 | 0.08 | 11.50 - 11.94 | 11.64 |
| unidentified | 147984.13 | | | 0.11 | 11.94 - 12.47 | 12.32 |
| A2G1F/A2S2F_0K | 148153.43 | 148143.92 | 64.2 | 0.05 | 11.87 - 12.42 | 12.17 |
| A2G2F/A2S2F_0K | 148304.16 | 148306.06 | -12.8 | 0.02 | 11.94 - 12.42 | 12.17 |
| unidentified | 148450.58 | | | 0.03 | 11.79 - 12.32 | 12.01 |
| A2S1G1F/A2S2F_0K | 148588.03 | | | 0.01 | 11.50 - 12.47 | 11.64 |
| M5_1K | 145538.00 | 145529.58 | 57.9 | 0.01 | 12.84 - 13.34 | 13.20 |
| A2G0F_1K | 145761.47 | 145757.82 | 25.0 | 0.16 | 12.68 - 13.34 | 13.20 |
| A2G1F_1K | 145921.64 | 145919.96 | 11.5 | 0.15 | 12.58 - 13.34 | 13.20 |
| A2G2F_1K | 146081.62 | 146082.10 | -3.3 | 0.07 | 12.74 - 13.34 | 13.20 |
| unidentified | 146234.50 | | | 0.08 | 12.58 - 13.34 | 13.20 |
| unidentified | 146384.86 | | | 0.10 | 12.58 - 13.34 | 13.11 |
| unidentified | 146539.10 | | | 1.08 | 12.58 - 13.34 | 13.20 |
| unidentified | 146700.72 | | | 0.27 | 12.68 - 13.19 | 12.83 |
| unidentified | 146864.86 | | | 0.13 | 12.58 - 13.12 | 12.89 |
| A2G0/A2G0F_1K | 147055.78 | 147057.02 | -8.4 | 3.22 | 12.74 - 13.34 | 13.20 |
| A2G0F/A2G0F_1K | 147206.07 | 147203.16 | 19.8 | 28.55 | 12.68 - 13.34 | 13.20 |
| A2G0F/A2G1F_1K | 147367.02 | 147365.30 | 11.7 | 39.42 | 12.58 - 13.34 | 13.20 |
| A2G1F/A2G1F_1K or A2G0F/A2G2F_1K | 147529.70 | 147527.44 | 15.3 | 21.79 | 12.58 - 13.34 | 13.20 |
| A2G1F/A2G2F_1K | 147694.70 | 147689.58 | 34.7 | 4.43 | 12.58 - 13.34 | 13.20 |
| A2G2F/A2G2F_1K | 147851.95 | 147851.72 | 1.5 | 0.25 | 12.58 - 13.34 | 12.73 |
| A2G1F/A2S1G1F_1K | 147995.66 | 147980.84 | 100.2 | 0.03 | 12.68 - 13.26 | 12.83 |
| A2G2F/A2S1G1F_1K | 148133.03 | 148142.98 | -67.1 | 0.04 | 12.74 - 13.19 | 12.98 |
| unidentified | 148252.85 | | | 0.06 | 12.89 - 13.34 | 13.20 |
| unidentified | 148407.37 | | | 0.12 | 12.58 - 13.34 | 13.20 |
| unidentified | 148572.29 | | | 0.04 | 12.84 - 13.34 | 13.20 |
| unidentified | 145739.58 | | | 0.02 | 14.49 - 15.15 | 14.96 |
| A2G0F_2K | 145888.38 | 145886.00 | 16.4 | 0.17 | 14.23 - 15.15 | 14.77 |
| A2G1F_2K | 146048.16 | 146048.14 | 0.1 | 0.12 | 14.49 - 15.15 | 14.96 |
| A2G2F_2K | 146203.22 | 146210.28 | -48.3 | 0.02 | 14.59 - 15.15 | 14.96 |
| unidentified | 146353.75 | | | 0.06 | 14.38 - 15.15 | 14.96 |
| unidentified | 146524.81 | | | 0.09 | 14.23 -15.15 | 14.41 |
| unidentified | 146670.63 | | | 0.25 | 14.23 - 15.05 | 14.41 |
| M5/M5_2K | 146877.43 | 146874.84 | 17.6 | 0.39 | 14.59 - 15.15 | 14.96 |
| A2G0/A2G0_2K | 147038.77 | 147039.05 | -1.9 | 0.09 | 14.49 - 15.05 | 14.77 |
| A2G0/A2G0F_2K | 147186.12 | 147185.19 | 6.3 | 3.98 | 14.28 - 15.15 | 14.96 |
| A2G0F/A2G0F_2K | 147334.13 | 147331.33 | 19.0 | 32.55 | 14.23 - 15.15 | 14.96 |
| A2G0F/A2G1F_2K | 147495.66 | 147493.47 | 14.8 | 38.86 | 14.23 - 15.15 | 14.87 |
| A2G1F/A2G1F_2K or A2G0F/A2G2F_2K | 147656.06 | 147655.61 | 3.0 | 19.50 | 14.23 - 15.15 | 14.87 |
| A2G1F/A2G2F_2K | 147821.64 | 147817.75 | 26.3 | 3.69 | 14.23 - 15.15 | 14.77 |
| A2G2F/A2G2F_2K | 147990.79 | 147979.89 | 73.6 | 0.11 | 14.28 - 15.15 | 14.96 |

**Table S5.** Glycoform annotation the deconvoluted mass spectrum of Reditux™ after carboxypeptidase B (CpB) treatment (Figure 1h and Figure 4) reporting variant name, experimental mass, theoretical mass, mass deviation in ppm, fractional abundance, retention time range and retention time apex. Theoretical masses were calculated considering N-terminal pyro-Glu as a fixed modification. Glycan structures, names and compositions are collected in Table S1.

| | Reditux™ CpB annotation | | | | | |
|---|---|---|---|---|---|---|
| Variant Name | Experimental Mass [Da] | Theoretical Mass [Da] | Mass deviation [ppm] | Fractional Abundance [%] | RT range [min] | RT apex [min] |
| M5_0K | 145404.26 | 145401.40 | 19.6 | 0.02 | 10.55 - 11.96 | 11.61 |
| A2G0F_0K | 145633.35 | 145629.65 | 25.4 | 0.17 | 10.18 - 11.96 | 11.61 |
| A2G1F_0K | 145793.11 | 145791.79 | 9.1 | 0.15 | 9.66 - 11.96 | 11.61 |
| A2G2F_0K | 145951.96 | 145953.93 | -13.5 | 0.02 | 9.50 - 11.60 | 11.06 |
| A2S1G0F_0K | 146095.07 | 146083.05 | 82.3 | 0.04 | 10.71 - 11.96 | 11.61 |
| unidentified | 146259.78 | | | 0.01 | 10.39 - 11.96 | 11.61 |
| M5/M5_0K | 146620.20 | 146618.49 | 11.6 | 1.60 | 9.50 - 11.96 | 11.61 |
| A2G0/A2G0_0K | 146783.34 | 146782.70 | 4.3 | 0.14 | 9.50 - 11.41 | 10.90 |
| A2G0/A2G0F_0K | 146929.03 | 146928.84 | 1.2 | 3.71 | 9.50 - 11.96 | 11.61 |
| A2G0F/A2G0F_0K | 147077.87 | 147074.99 | 19.6 | 26.82 | 9.50 - 11.96 | 11.61 |
| A2G0F/A2G1F_0K | 147237.46 | 147237.13 | 2.3 | 35.28 | 9.50 - 11.96 | 11.61 |
| A2G1F/A2G1F_0K or A2G0F/A2G2F_0K | 147398.63 | 147399.27 | -4.3 | 23.02 | 9.66 - 11.96 | 11.61 |
| A2G1F/A2G2F_0K | 147561.06 | 147561.41 | -2.3 | 6.92 | 9.50 - 11.96 | 11.61 |
| A2G2F/A2G2F_0K | 147715.68 | 147723.55 | -53.3 | 0.61 | 10.39 - 11.60 | 11.06 |
| A2G1F/A2S1G1F_0K | 147857.54 | 147852.66 | 33.0 | 0.31 | 10.18 - 11.60 | 10.90 |
| A2G2F/A2S1G1F_0K | 148003.91 | 148014.80 | -73.6 | 0.12 | 9.50 - 11.07 | 10.36 |
| A2G1F/A2S2F_0K | 148150.60 | 148143.92 | 45.1 | 0.15 | 9.66 - 11.96 | 10.55 |
| A2G2F/A2S2F_0K | 148310.86 | 148306.06 | 32.4 | 0.05 | 9.50 - 11.25 | 10.55 |
| unidentified | 148843.50 | | | 0.02 | 9.87 - 11.96 | 11.61 |

**Table S6.** Basic variant annotation of deconvoluted mass spectrum of Reditux™ after carboxypeptidase B (CpB) treatment (Figure 1i) reporting variant name, experimental mass, theoretical mass, mass deviation in ppm, fractional abundance, retention time range and retention time apex. The basic variant arising from N-terminal cleavage of residues Q1-S5 of the light chain (Figure S1) is indicated as (LC pyro-Glu (Q6) - N-term Q1-S5). Unidentified basic PTMs could be attributed to some modifications with a basic nature not-resolvable by MS at intact level, e.g C-terminal proline amidation, succinimide formation, methionine oxidation, glutamic acid instead of pyro-glutamate, isomerization of aspartate, disulfide shuffling. Glycan structures, names and compositions are collected in Table S1.

**Reditux™ CpB basic variant annotation, RT range (12.00-17.00 min)**

| Variant Name | Experimental Mass [Da] | Theoretical Mass [Da] | Mass deviation [ppm] | Fractional Abundance [%] | RT range [min] | RT apex [min] |
|---|---|---|---|---|---|---|
| Unidentified basic PTM | 145300.43 | | | 0.03 | 14.02 - 15.39 | 14.68 |
| Unidentified basic PTM + M5_0K | 145404.36 | | | 0.08 | 11.99 - 14.23 | 12.46 |
| Unidentified basic PTM + A2G0F_0K | 145636.57 | | | 0.24 | 11.99 - 14.50 | 12.46 |
| Unidentified basic PTM + A2G1F_0K | 145791.17 | | | 0.18 | 11.99 - 14.50 | 12.46 |
| M5/M5_0K (LC pyro-Glu (Q6) - N-term Q1-S5) | 146094.49 | 146076.86 | 120.7 | 0.23 | 11.99 - 14.23 | 12.46 |
| A2G0/A2G0F_0K (LC pyro-Glu (Q6) - N-term Q1-S5) | 146390.07 | 146387.21 | 19.6 | 0.53 | 12.24 - 14.23 | 13.10 |
| A2G0F/A2G0F_0K (LC pyro-Glu (Q6) - N-term Q1-S5) | 146538.93 | 146533.35 | 38.1 | 3.75 | 12.45 - 14.71 | 13.37 |
| A2G0F/A2G1F_0K (LC pyro-Glu (Q6) - N-term Q1-S5) | 146698.59 | 146695.49 | 21.1 | 4.09 | 12.24 - 14.92 | 13.37 |
| A2G1F/A2G1F_0K (LC pyro-Glu (Q6) - N-term Q1-S5) | 146859.13 | 146857.63 | 10.2 | 1.61 | 12.45 - 14.02 | 13.10 |
| Unidentified basic PTM + A2G0/A2G0F_0K | 146929.23 | | | 0.74 | 13.34 - 16.96 | 14.26 |
| Unidentified basic PTM + A2G0F/A2G0F_0K | 147080.44 | | | 27.51 | 11.99 - 16.96 | 12.46 |
| Unidentified basic PTM + A2G0F/A2G1F_0K | 147244.84 | | | 21.00 | 11.99 - 13.34 | 12.46 |
| Unidentified basic PTM + A2G1F/A2G1F_0K or A2G0F/A2G2F_0K | 147405.01 | | | 10.17 | 11.99 - 13.34 | 12.46 |
| Unidentified basic PTM + A2G1F/A2G2F_0K | 147564.80 | | | 3.81 | 11.99 - 16.96 | 12.46 |
| Unidentified basic PTM + A2G2F/A2G2F_0K | 147722.76 | | | 0.50 | 12.66 - 16.28 | 14.26 |
| Unidentified basic PTM + A2G1F/A2S1G1F_0K | 147855.66 | | | 0.09 | 12.24 - 14.92 | 12.69 |

**Table S7.** Results of fractional abundance semi-quantitation of MabThera® and Reditux™ glycoforms via Extracted ion current chromatograms (EICCs) integration using Fragquaxi. CpB indicates the treatment with carboxypeptidase. Bar charts referred to MabThera® vs Reditux™ CpB and Reditux™ 0K, 1K and 2K can be found in the main manuscript (Figure 5). Glycan structures, names and compositions are collected in Table S1.

| | MabThera® CpB | | Reditux™ CpB | | MabThera® | | Reditux™ 0K | | Reditux™ 1K | | Reditux™ 2K | |
|---|---|---|---|---|---|---|---|---|---|---|---|---|
| Glycoforms | Average [%] | STD [%] | Average [%] | STD [%] | Average [%] | STD [%] | Average [%] | STD [%] | Average [%] | STD [%] | Average [%] | STD [%] |
| M5 | 0.03 | 0.01 | 0.08 | 0.00 | 0.04 | 0.02 | 0.14 | 0.01 | 0.06 | 0.01 | 0.10 | 0.03 |
| A2G0F | 0.31 | 0.00 | 0.30 | 0.01 | 0.31 | 0.01 | 0.31 | 0.00 | 0.31 | 0.01 | 0.29 | 0.02 |
| A2G1F | 0.42 | 0.01 | 0.27 | 0.00 | 0.42 | 0.00 | 0.30 | 0.01 | 0.26 | 0.01 | 0.23 | 0.01 |
| A2G2F | 0.12 | 0.01 | 0.08 | 0.01 | 0.12 | 0.01 | 0.12 | 0.01 | 0.20 | 0.01 | 0.11 | 0.01 |
| A2S1G0F | 0.03 | 0.01 | 0.13 | 0.01 | 0.04 | 0.02 | 0.15 | 0.01 | 0.12 | 0.00 | 0.13 | 0.00 |
| M5/M5 | 0.50 | 0.01 | 2.30 | 0.02 | 0.45 | 0.01 | 3.24 | 0.03 | 1.07 | 0.02 | 0.93 | 0.02 |
| A2G0/M5 | 0.27 | 0.07 | 0.58 | 0.03 | 0.38 | 0.01 | 0.18 | 0.01 | 0.67 | 0.04 | 0.98 | 0.07 |
| A2G0F/M5 | 0.57 | 0.04 | 0.86 | 0.03 | 0.64 | 0.04 | 0.82 | 0.01 | 0.43 | 0.02 | 1.08 | 0.11 |
| A2G1/M5 | 0.62 | 0.04 | 0.88 | 0.03 | 0.70 | 0.04 | 0.78 | 0.01 | 0.39 | 0.02 | 0.64 | 0.06 |
| A2G0/A2G0 | 0.01 | 0.00 | 0.80 | 0.01 | 0.02 | 0.01 | 1.06 | 0.02 | 0.55 | 0.10 | 0.81 | 0.04 |
| A2G0F/A2G0 | 0.47 | 0.01 | 4.28 | 0.03 | 0.44 | 0.01 | 4.04 | 0.05 | 6.41 | 0.45 | 5.63 | 0.03 |
| A2G0F/A2G0F | 19.87 | 0.21 | 27.13 | 0.15 | 19.70 | 0.26 | 24.33 | 0.15 | 28.63 | 0.31 | 28.13 | 0.42 |
| A2G0F/A2G1F | 33.50 | 0.17 | 34.93 | 0.06 | 33.40 | 0.17 | 33.17 | 0.23 | 35.00 | 0.30 | 35.37 | 0.25 |
| A2G1F/A2G1F | 28.20 | 0.00 | 20.10 | 0.10 | 28.20 | 0.10 | 20.90 | 0.10 | 19.13 | 0.06 | 19.13 | 0.06 |
| A2G1F/A2G2F | 10.73 | 0.06 | 5.55 | 0.08 | 10.80 | 0.10 | 6.83 | 0.21 | 4.90 | 0.03 | 4.77 | 0.07 |
| A2G2F/A2G2F | 2.15 | 0.03 | 0.92 | 0.01 | 2.15 | 0.05 | 1.66 | 0.06 | 0.86 | 0.04 | 0.79 | 0.06 |
| A2G1F/A2S1G1F | 1.04 | 0.09 | 0.38 | 0.02 | 1.08 | 0.13 | 1.01 | 0.01 | 0.45 | 0.03 | 0.33 | 0.04 |
| A2G1F/A2S2F | 0.41 | 0.04 | 0.15 | 0.01 | 0.45 | 0.05 | 0.33 | 0.01 | 0.15 | 0.02 | 0.19 | 0.06 |
| A2G2F/A2S1G1F | 0.45 | 0.04 | 0.17 | 0.01 | 0.45 | 0.06 | 0.43 | 0.02 | 0.21 | 0.03 | 0.22 | 0.06 |
| A2G2F/A2S2F | 0.25 | 0.03 | 0.09 | 0.01 | 0.27 | 0.04 | 0.22 | 0.04 | 0.13 | 0.03 | 0.16 | 0.04 |

**Table S8.** Optimized deconvolution parameters used in BioPharma Finder™ 3.0 for the mass spectra of MabThera® and Reditux™ before and after carboxypeptidase treatment (CpB).

| Deconvolution Parameters BioPharma Finder 3.0 | | | | | | | | | |
|---|---|---|---|---|---|---|---|---|---|
| | | Parameter | MabThera® | MabThera® CpB | Reditux™ 0K | Reditux™ 1K | Reditux™ 2K | Reditux™ CpB | Reditux™ CpB basic variants |
| Chromatogram and Source Spectra | Chromatogram Parameters | *m/z* range | 2500-8000 | | 5000-7000 | | | 2500-8000 | |
| | Source spectra method | | sliding window | | | | | | |
| | Sliding Windows Definition | RT Range [mim] | 9.00-12.00 | 9.00-12.00 | 11.50-12-50 | 12.60-13-40 | 14.20-15-20 | 9.50-12-00 | 12.00-17.00 |
| | | Target Avg Spectrum Width [min] | 1.000 | 0.480 | 0.300 | 0.300 | 0.380 | 0.700 | 0.900 |
| | | Target Avg Spectrum % Offset | 25 | | | | | | |
| | Sliding Windows Merging Parameters | Merge Tolerance [ppm] | 20 | | | | | | |
| | | Max RT Gap [min] | 1 | | | | | | |
| | | Min. Number of Detected Intervals | 3 | | | | | | |
| Deconvolution Algorithm, basic | Deconvolution Results Filter | Output Mass Range | 145000-149000 | | | | | | |
| | | Deconvolution Spectra Display Mode | Isotopic Profile | | | | | | |
| | Charge State Distribution | Deconvolution Mass Tolerance [ppm] | 20 | | | | | | |
| | Choice of Peak Model | Choice of Peak Model | Intact Protein | | | | | | |
| | | Resolution at 400 *m/z* | Raw File Specific | | | | | | |
| Deconvolution Algorithm, advanced | Deconvolution Algorithm | | ReSpect™ | | | | | | |
| | Charge State Distribution | Model Mass Range | 145000-149000 | | | | | | |
| | | Charge State Range | 20-28 | | 23-27 | | | | |
| | | Minimum Adjacent Charges (low and high model mass) | 2 to 2 | | | | | | |
| | Noise Parameters | Rel. Abundance Threshold (%) | 0.00 | | | | | | |
| | Deconvolution Quality | Quality Score Threshold | 0.00 | | | | | | |
| | Choice of Peak Model | Target Mass | 147000 | | | | | | |
| | Peak Model Parameters | Number of Peak Models | 1 | | | | | | |
| | | Left/Right Peak Shape | Left 2.00, Right 2.00 | | | | | Left 2.00, Right 3.00 | Left 2.00, Right 2.00 |
| | Peak Filter Parameters | Peak Detection Minimum Significance Measure | 1.00 | | 1.50 | | | 1.00 | |
| | | Peak Detection Quality Measure [%] | 95 | | | | | | |
| | Specialized Parameters | Peak Model Width Factor | 1.00 | | 1.80 | | | 1.50 | |
| | | Intensity Threshold Scale | 0.00001 | | | | | | |
| | Deconvolution Parameters | Noise Compesation | ✓ | | | | | | |
| | | Charge Carrier | H+ | | | | | | |